Available online at www.sciencedirect.com
SCIENCE DIRECT
Journal of Sound and Vibration 297 (2006) 293–314
JOURNAL OF SOUND AND VIBRATION
www.elsevier.com/locate/jsvi

Finite cylinder vibrations with different end boundary conditions

M.R. Mofakhami[a], H.H. Toudeshky[a,*], Sh.H. Hashemi[b]

[a]*Aerospace Engineering Department, Amirkabir University of Technology (Tehran Polytechnic), 424, Hafez Avenue, Tehran 158754413, Iran*
[b]*School of Mechanical Engineering, Iran University of Science and Technology, Narmak, Tehran, Iran*

Received 21 September 2005; received in revised form 22 March 2006; accepted 30 March 2006
Available online 8 June 2006

Abstract

Utilizing the infinite circular cylinders solution based on the technique of variables separation, a general solution is developed to analyze the vibration of finite circular cylinders. The vibration of finite circular cylinders with different end boundary conditions as well as the curved panels can be analyzed by the semi-analytical method developed in the present study. In the present paper two different boundary conditions are considered, namely the free-end and fixed-end hollow cylinders. Convergence and precision of the method are determined to calculate the natural frequencies of various geometrical configurations. It is shown that the results obtained from the present semi-analytical method are in good agreement with those obtained using the previously developed methods. Generality, high accuracy and good convergence with a small sized of coefficient matrix are the merits of the present method.

1. Introduction

Finite length hollow cylinders are indispensable in many industries such as marine structures, necessitating the thorough comprehension of their vibration with different boundary conditions. These understanding may be used to analyze the sound transmission through the single and multilayered finite cylinders. The earliest investigation concerning the vibration of cylinders was performed by Pochhamer [1] and Chree [2]. The Pochhamer–Chree solution was developed for an infinitely long solid cylinder. Greenspon [3], Gazis [4] and Armenakas [5] studied the vibration of infinitely long traction free hollow cylinders using linear three dimensional (3D) theory of elasticity. McNevin et al. [6] developed a three-mode theory for axisymmetric vibrations of rods and hollow cylinders. Gladwell and Tahbildar [7] investigated axisymmetric vibrations of cylinders using the finite-element method. The vibration of free finite length circular cylinders using the finite-element method was analyzed by Gladwell and Vijay [8]. Hutchinson [9,10] developed a semi-analytical highly accurate method to solve the vibrations of finite length rods and solid cylinders on the basis of linear 3D elasticity. Hutchinson and El-Azhari [11] investigated the vibrations of free hollow finite length circular

*Corresponding author. Tel.: +98 21 6454 3224; fax: +98 21 66404885.
E-mail addresses: Mofakhami@aut.ac.ir (M.R. Mofakhami), Hosseini@aut.ac.ir (H.H. Toudeshky), Shh@iust.ac.ir (S.H. Hashemi).

0022-460X/$ - see front matter
doi:10.1016/j.jsv.2006.03.041

Nomenclature

a, b	inner and outer radii of the cylinder
A_k, B_k, F_k, G_k, $\bar{F}_k$,$\bar{G}_k$,	constants
C_1, C_2	propagation velocity of dilatational and distortional waves
H	ratio of the thickness with respect to the mean radius
$\mathbf{H}$	vector potential functions
I_v, K_v	modified Bessel functions (order v)
J_v, Y_v	bessel and Neumann functions (order v)
l	half length of the cylinder
L	ratio of the length over the mean radius
n	circumferential wave number
N_1, N_2	number of truncated series terms in z and r directions
r, θ, z	cylindrical coordinates
t	time
$\mathbf{u}$	displacement vector
λ, μ	lame constants
ρ	density
$\boldsymbol{\sigma}$	stress field
φ	scalar potential functions
ω	circular frequency
$\Omega = \omega b/C_2$	non-dimensional natural frequency
∇^2	three-dimensional Laplacian operator

cylinders using the method which had been previously reported by Hutchinson. In Hutchinson's heretofore studies different forms of solutions, by combining some fundamental solution forms are suggested for the above mentioned cases. Singal and Williams [12] investigated the vibrations of thick hollow cylinders using the energy method based on the 3D theory of elasticity. Leissa and So [13,14] studied the vibrations of free and cantilevered solid cylinders using simple algebraic polynomials in the Ritz method. Liew et al. [15–17] studied the free vibrations of solid and hollow cylinders with different end boundary conditions using 3D energy displacement-based expressions. The convergence of the method and parametric investigations were performed for different boundary conditions and cross-sections of hollow cylinders. Some studies have also been performed on the vibrations of the cylinders that include the classification of natural frequencies or mode shapes such as the one presented by Wang and Williams [18] using the finite element method. Modified methods are also used to obtain more accurate and better convergence of the results, for example Zhou et al. [19] studied 3D vibrations of the solid and hollow cylinders using the Ritz method and Chebyshev polynomials.

In this paper a general semi-analytical solution using the technique of variables separation on the basis of linear 3D theory of elasticity is developed which covers different cases of finite length cylinders such as rods, solid cylinders, hollow cylinders and curved panels with various boundary conditions. In this method some of the boundary conditions need to be approximately satisfied using orthogonalization technique while the others to be exact. Comparing with the previously developed series solutions, high accuracy and good convergence with a small sized of coefficient matrix are achieved in the eigenvalues estimation using the present method.

2. Formulation

The geometry of a typical hollow circular cylinder is shown in Fig. 1. An orthogonal cylindrical coordinate (r, θ, z) system is considered as shown in this figure. The corresponding components of the displacement vector $\mathbf{u}$ at a point are u_r, u_θ and u_z in the r, θ, and z directions, respectively. The displacement equations governing the motion of an isotropic media are

$$\rho \frac{\partial^2 \mathbf{u}}{\partial t^2} = \mu \nabla^2 \mathbf{u} + (\lambda + \mu) \nabla (\nabla . \mathbf{u}), \tag{1}$$

where ρ is the density, λ and μ are the Lame constants, and ∇^2 is the 3D Laplacian operator. The most general solution of Eq. (1) may be obtained using Helmholtz decomposition as follows:

$$\mathbf{u} = \nabla \varphi + \nabla \times \mathbf{H} \tag{2}$$

with the condition of

$$\nabla . \mathbf{H} = F(r, \theta, z, t), \tag{3}$$

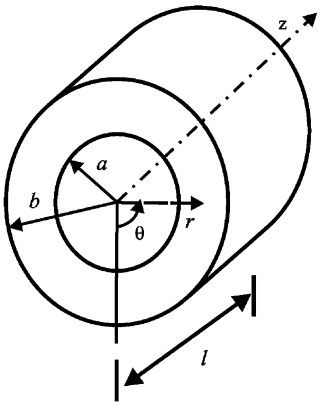

Fig. 1. A half hollow circular cylinder configuration.

where φ and $\mathbf{H}$ are scalar and vector potential functions respectively and F is an arbitrary function that may be taken as zero [5]. Substituting $\mathbf{u}$ from Eq. (2) into Eq. (1) results the following wave equations:

$$C_1^2\nabla^2\varphi = \frac{\partial^2\varphi}{\partial t^2},$$
$$C_2^2\nabla^2\mathbf{H} = \frac{\partial^2\mathbf{H}}{\partial t^2}, \tag{4}$$

where

$$C_1 = \sqrt{\frac{\lambda+2\mu}{\rho}},$$
$$C_2 = \sqrt{\frac{\mu}{\rho}}. \tag{5}$$

The constants C_1 and C_2 are the propagation velocity of dilatational and distortional waves in an infinite medium, respectively. Employing the technique of variables separation the following general solutions in cylindrical coordinates can be obtained

$$\begin{aligned}
\varphi(r,\theta,z,t) &= \left[R_1(\alpha_1 r)T_1(\delta_1 z) + \bar{R}_1(\bar{\alpha}_1 r)T_1(\bar{\delta}_1 z)\right]E_1(v\theta)\mathrm{e}^{\mathrm{i}\omega t},\\
H_r(r,\theta,z,t) &= \left[R_2(\alpha_{23} r)T_2(\delta_{23} z) + \bar{R}_2(\bar{\alpha}_{23} r)T_2(\bar{\delta}_{23} z)\right]E_2(v\theta)\mathrm{e}^{\mathrm{i}\omega t},\\
H_\theta(r,\theta,z,t) &= \left[R_3(\alpha_{23} r)T_3(\delta_{23} z) + \bar{R}_3(\bar{\alpha}_{23} r)T_3(\bar{\delta}_{23} z)\right]E_3(v\theta)\mathrm{e}^{\mathrm{i}\omega t},\\
H_z(r,\theta,z,t) &= \left[R_4(\alpha_4 r)T_4(\delta_4 z) + \bar{R}_4(\bar{\alpha}_4 r)T_4(\bar{\delta}_4 z)\right]E_4(v\theta)\mathrm{e}^{\mathrm{i}\omega t},
\end{aligned} \tag{6}$$

where

$$\begin{aligned}
R_1(\alpha_1 r) &= F_1 J_v(\alpha_1 r) + G_1 Y_v(\alpha_1 r),\\
R_2(\alpha_{23} r) &= F_2 J_{v+1}(\alpha_{23} r) + G_2 Y_{v+1}(\alpha_{23} r) + \frac{v}{\alpha_{23} r}[(F_3 - F_2)J_v(\alpha_{23} r) + (G_3 - G_2)Y_v(\alpha_{23} r)],\\
R_3(\alpha_{23} r) &= F_3 J_{v+1}(\alpha_{23} r) + G_3 Y_{v+1}(\alpha_{23} r) + \frac{v}{\alpha_{23} r}[(F_2 - F_3)J_v(\alpha_{23} r) + (G_2 - G_3)Y_v(\alpha_{23} r)],\\
R_4(\alpha_4 r) &= F_4 J_v(\alpha_4 r) + G_4 Y_v(\alpha_4 r),
\end{aligned}$$

$$\delta_1^2 + \alpha_1^2 = \bar{\delta}_1^2 + \bar{\alpha}_1^2 = \left(\frac{\omega^2}{C_1^2}\right),$$
$$\delta_{23}^2 + \alpha_{23}^2 = \bar{\delta}_{23}^2 + \bar{\alpha}_{23}^2 = \left(\frac{\omega^2}{C_2^2}\right),$$

$$\delta_4^2 + \alpha_4^2 = \bar{\delta}_4^2 + \bar{\alpha}_4^2 = \left(\frac{\omega^2}{C_2^2}\right), \tag{7}$$

$$T_1(\delta_1 z) = \begin{Bmatrix} \cos(\delta_1 z) \\ \sin(\delta_1 z) \end{Bmatrix}, \quad T_2(\delta_{23} z) = \begin{Bmatrix} \sin(\delta_{23} z) \\ \cos(\delta_{23} z) \end{Bmatrix},$$

$$T_3(\delta_{23} z) = \begin{Bmatrix} -\sin(\delta_{23} z) \\ \cos(\delta_{23} z) \end{Bmatrix}, \quad T_4(\delta_4 z) = \begin{Bmatrix} \cos(\delta_4 z) \\ \sin(\delta_4 z) \end{Bmatrix},$$

$$E_1(v\theta) = E_3(v\theta) = \begin{Bmatrix} \cos(v\theta) \\ \sin(v\theta) \end{Bmatrix}, \quad E_2(v\theta) = E_4(v\theta) = \begin{Bmatrix} \sin(v\theta) \\ \cos(v\theta) \end{Bmatrix}$$

and J_v and Y_v denote the Bessel and Neumann functions for real arguments, or will be replaced by I_v and K_v for imaginary arguments, v is a real number, F_k and G_k ($k = 1, 2, 3, 4$) are the constants and ω is the circular frequency. The second terms in Eq. (6) are added to satisfy the end boundary conditions. The functions of $\bar{R}_k(\bar{\alpha} r)$ and $T_k(\bar{\delta} z)$ ($k = 1, 2, 3, 4$) can be calculated using $\bar{\alpha}$ and $\bar{\delta}$ in Eq. (7) instead of α and δ, respectively. This general solution for potential functions may be used to analyze the wave propagation in infinite or finite circular cylinders and curved panels. In comparison with those investigated by Gazis [4] for infinite circular cylinders, the above solution provides more coefficients to evaluate the wave propagation in the finite circular cylinders and curved panels with different end boundary conditions. Comparing with the before mentioned Hutchinson's studies on the vibration of free-end circular cylinders, additional terms have been included to the solution of the infinite cylinders.

In this paper two different boundary conditions are considered. At first the free-end hollow circular cylinder is analyzed to verify the obtained results with those performed by Hutchinson and El-Azhari [11], So and Leissa [14] and Zhou et al. [19]. Then the fixed-end hollow circular cylinder is analyzed to present the combination of the displacement and stress boundary conditions. The fixed-end hollow circular cylinder is more applicable in design and analysis of industrial problems such as the analysis of the coupled structure-acoustic models. The results obtained may be affected by scattering and transmission of sound through the open end as provided by Lee and Kim [20]. To avoid this, the fixed-end boundary conditions are chosen in the experiments. In addition the present method can be used to evaluate the wave propagation in the curved panels, which will be investigated in future work.

If an isotropic elastic circular cylinder with the inner and outer radii of a and b and finite length of $2l$ is considered, the generalized solution form (6) is reduced to a simple form with 12 independent terms by identifying the variables as follows:

$$\begin{aligned} &v = n, \\ &\delta_2 = \delta_{23} = \delta_4, \\ &\alpha = \alpha_1 = \alpha_2 = \alpha_{23} = \alpha_4, \\ &\bar{\delta} = \bar{\delta}_1 = \bar{\delta}_2 = \bar{\delta}_{23} = \bar{\delta}_4, \\ &\bar{\alpha}_2 = \bar{\alpha}_{23} = \bar{\alpha}_4, \end{aligned} \tag{8}$$

where n is circumferential wave number. Substituting from Eq. (8) into Eq. (6), and the resultant equation into Eq. (2) leads to the following displacement components:

$$\begin{aligned} u_r = &\left\{ \left[\left(\frac{n}{r} J_n(\alpha r) - \alpha J_{n+1}(\alpha r)\right) A_1 + \left(\frac{n}{r} Y_n(\alpha r) - \alpha Y_{n+1}(\alpha r)\right) B_1 \right] \begin{Bmatrix} \cos(\delta_1 z) \\ \sin(\delta_1 z) \end{Bmatrix}, \right. \\ &\left. + \left[\delta_2 J_{n+1}(\alpha r) A_2 + \delta_2 Y_{n+1}(\alpha r) B_2 + \left\{ \frac{n}{r} J_n(\alpha r) A_3 + \frac{n}{r} Y_n(\alpha r) B_3 \right\} \begin{Bmatrix} 1 \\ -1 \end{Bmatrix} \right] \begin{Bmatrix} \cos(\delta_2 z) \\ \sin(\delta_2 z) \end{Bmatrix} \right. \end{aligned}$$

$$+\left[\left(\frac{n}{r}J_n(\bar{\alpha}_1 r)-\bar{\alpha}_1 J_{n+1}(\bar{\alpha}_1 r)\right)A_4+\left(\frac{n}{r}Y_n(\bar{\alpha}_1 r)-\bar{\alpha}_1 Y_{n+1}(\bar{\alpha}_1 r)\right)B_4+\bar{\delta}J_{n+1}(\bar{\alpha}_2 r)A_5\right.$$
$$\left.+\bar{\delta}Y_{n+1}(\bar{\alpha}_2 r)B_5+\left\{\frac{n}{r}J_n(\bar{\alpha}_2 r)A_6+\frac{n}{r}Y_n(\bar{\alpha}_2 r)B_6\right\}\begin{Bmatrix}1\\-1\end{Bmatrix}\right]\begin{Bmatrix}\cos(\bar{\delta}z)\\\sin(\bar{\delta}z)\end{Bmatrix}\Bigg\}\begin{Bmatrix}\cos(n\theta)\\\sin(n\theta)\end{Bmatrix}e^{i\omega t},$$

$$u_\theta=\left\{\left[-\frac{n}{r}J_n(\alpha r)A_1-\frac{n}{r}Y_n(\alpha r)B_1\right]\begin{Bmatrix}1\\-1\end{Bmatrix}\begin{Bmatrix}\cos(\delta_1 z)\\\sin(\delta_1 z)\end{Bmatrix}\right.$$
$$+\left[[\delta_2 J_{n+1}(\alpha r)A_2+\delta_2 Y_{n+1}(\alpha r)B_2]\begin{Bmatrix}1\\-1\end{Bmatrix}-\left(\frac{n}{r}J_n(\alpha r)-\alpha J_{n+1}(\alpha r)\right)A_3\right.$$
$$\left.-\left(\frac{n}{r}Y_n(\alpha r)-\alpha Y_{n+1}(\alpha r)\right)B_3\right]\begin{Bmatrix}\cos(\delta_2 z)\\\sin(\delta_2 z)\end{Bmatrix}+\left[\left\{-\frac{n}{r}J_n(\bar{\alpha}_1 r)A_4-\frac{n}{r}Y_n(\bar{\alpha}_1 r)B_4\right.\right.$$
$$\left.+\bar{\delta}J_{n+1}(\bar{\alpha}_2 r)A_5+\bar{\delta}Y_{n+1}(\bar{\alpha}_2 r)B_5\right\}\begin{Bmatrix}1\\-1\end{Bmatrix}-\left(\frac{n}{r}J_n(\bar{\alpha}_2 r)-\bar{\alpha}_2 J_{n+1}(\bar{\alpha}_2 r)\right)A_6$$
$$\left.\left.-\left(\frac{n}{r}Y_n(\bar{\alpha}_2 r)-\bar{\alpha}_2 Y_{n+1}(\bar{\alpha}_2 r)\right)B_6\right]\begin{Bmatrix}\cos(\bar{\delta}z)\\\sin(\bar{\delta}z)\end{Bmatrix}\right\}\begin{Bmatrix}\sin(n\theta)\\\cos(n\theta)\end{Bmatrix}e^{i\omega t} \tag{9}$$

$$u_z=-\left\{[\delta_1 J_n(\alpha r)A_1+\delta_1 Y_n(\alpha r)B_1]\begin{Bmatrix}\sin(\delta_1 z)\\\cos(\delta_1 z)\end{Bmatrix}+[\alpha J_n(\alpha r)A_2+\alpha Y_n(\alpha r)B_2]\begin{Bmatrix}\sin(\delta_2 z)\\\cos(\delta_2 z)\end{Bmatrix}\right.$$
$$+\left[\bar{\delta}J_n(\bar{\alpha}_1 r)A_4+\bar{\delta}Y_n(\bar{\alpha}_1 r)B_4+\bar{\alpha}_2 J_n(\bar{\alpha}_2 r)A_5\right.$$
$$\left.\left.+\bar{\alpha}_2 Y_n(\bar{\alpha}_2 r)B_5\right]\begin{Bmatrix}\sin(\bar{\delta}z)\\\cos(\bar{\delta}z)\end{Bmatrix}\right\}\begin{Bmatrix}1\\-1\end{Bmatrix}\begin{Bmatrix}\cos(n\theta)\\\sin(n\theta)\end{Bmatrix}e^{i\omega t},$$

where

$$A_1=F_1,A_2=F_3,A_3=F_4+\frac{\delta_2}{\alpha}(F_2-F_3)\begin{Bmatrix}1\\-1\end{Bmatrix},\quad B_1=G_1,B_2=G_3,B_3=G_4+\frac{\delta_2}{\alpha}(G_2-G_3)\begin{Bmatrix}1\\-1\end{Bmatrix},$$
$$A_4=\bar{F}_1,A_5=\bar{F}_3,A_6=\bar{F}_4+\frac{\bar{\delta}}{\bar{\alpha}_2}(\bar{F}_2-\bar{F}_3)\begin{Bmatrix}1\\-1\end{Bmatrix},\quad B_4=\bar{G}_1,B_5=\bar{G}_3,B_6=\bar{G}_4+\frac{\bar{\delta}}{\bar{\alpha}_2}(\bar{G}_2-\bar{G}_3)\begin{Bmatrix}1\\-1\end{Bmatrix}. \tag{10}$$

In light of Eqs. (9) and (10), two forms of symmetric and antisymmetric solutions are obtained Utilizing the strain–displacement and stress–strain relations, the relevant stress components can be obtained in a similar form as the displacement components that are given in Appendix A. The aforementioned displacement and stress fields satisfy the equilibrium equations, which confirms their validity. In the following sections, solutions of the hollow circular cylinders with two different boundary conditions are performed.

2.1. Free-end hollow circular cylinder

The boundary conditions of the free-end hollow circular cylinder are defined as follows:

$$\begin{aligned}&\sigma_{rr}=\sigma_{r\theta}=\sigma_{rz}=0\quad\text{at}\quad r=a,b,\\&\sigma_{zz}=\sigma_{rz}=\sigma_{\theta z}=0\quad\text{at}\quad z=-l,l.\end{aligned} \tag{11}$$

Exact satisfaction of the end boundary conditions for $a\leqslant r\leqslant b$ forces more than one relationship between the 12 independent coefficients presented in Eq. (9) and Appendix A. This implies that some of the boundary conditions should be approximately satisfied using the orthogonalization technique. Choosing which

boundary conditions are satisfied exactly and the others approximately is arbitrary. For example the following boundary conditions are satisfied exactly.

$$\begin{aligned} &\sigma_{rz} = 0 \qquad \text{at} \quad r = a, b, \\ &\sigma_{rz} = \sigma_{\theta z} = 0 \quad \text{at} \quad z = -l, l, \end{aligned} \tag{12}$$

And the other boundary conditions are satisfied using orthogonalization technique.

$$\begin{aligned} &\sigma_{rr} = \sigma_{r\theta} = 0 \quad \text{at} \quad r = a, b, \\ &\sigma_{zz} = 0 \qquad \text{at} \quad z = -l, l. \end{aligned} \tag{13}$$

For the sake of brevity of calculations, the first form of the solution "symmetric mode", is presented here. Satisfaction of the boundary conditions (12) leads to the following expressions:

$$\begin{aligned} &A_2 = -A_1 \frac{2\delta_1\alpha}{\alpha^2 - \delta_2^2} \frac{\sin(\delta_1 l)}{\sin(\delta_2 l)}, \quad B_2 = -B_1 \frac{2\delta_1\alpha}{\alpha^2 - \delta_2^2} \frac{\sin(\delta_1 l)}{\sin(\delta_2 l)}, \\ &A_3 = A_1 \frac{2\delta_1\delta_2}{\alpha^2 - \delta_2^2} \frac{\sin(\delta_1 l)}{\sin(\delta_2 l)}, \quad B_3 = B_1 \frac{2\delta_1\delta_2}{\alpha^2 - \delta_2^2} \frac{\sin(\delta_1 l)}{\sin(\delta_2 l)}, \\ &A_{5i} = \mathrm{K}_{1i} A_{4i} + \mathrm{K}_{2i} B_{4i} + \mathrm{K}_{3i} A_{6i} + \mathrm{K}_{4i} B_{6i}, \quad B_{5i} = \Lambda_{1i} A_{4i} + \Lambda_{2i} B_{4i} + \Lambda_{3i} A_{6i} + \Lambda_{4i} B_{6i}, \\ &\bar{\delta}_i = \frac{(i-1)\pi}{l} \quad i = 1, 2, 3, \ldots, \end{aligned} \tag{14}$$

where the coefficients K_{ki} and Λ_{ki} ($k = 1, 2, 3, 4$) are the functions of $\bar{\delta}_i, \bar{\alpha}_{1i}, \bar{\alpha}_{2i}$ and given in Appendix B. To apply the orthogonality on the second boundary conditions in Eq. (13), the following condition is considered:

$$J_n'(\alpha_j b) A_{1j} = -Y_n'(\alpha_j b) B_{1j}, \tag{15}$$

where prime denotes differentiation with respect to the relevant argument, α_j ($j = 1, 2, 3, \ldots$) is the root of $P_n'(\alpha_j a)$ and the orthogonal function $P_n(\alpha_j r)$ is defined as:

$$P_n(\alpha_j r) = Y_n'(\alpha_j b) J_n'(\alpha_j r) - J_n'(\alpha_j b) Y_n(\alpha_j r). \tag{16}$$

And the orthogonality can be demonstrated as follows

$$\int_a^b P_n(\alpha_j r) P_n(\alpha_k r) r \, \mathrm{d}r = \begin{cases} 0 & \text{for} \quad j \neq k, \\ \frac{1}{2}\left[\left(b^2 - a^2\right) + \frac{n^2\left(P_n^2(\alpha_j a) - P_n^2(\alpha_j b)\right)}{\alpha_j^2}\right] & \text{for} \quad j = k. \end{cases} \tag{17}$$

Therefore, the boundary conditions (13) are satisfied using orthogonalization as follows:

$$\begin{aligned} &\textstyle\int_a^b \sigma_{zz}(r, \theta, l) P_n(\alpha_j r) r \, \mathrm{d}r = 0, \\ &\textstyle\int_0^l \sigma_{rr}(r, \theta, z) \cos(\bar{\delta}_i z) \, \mathrm{d}z = 0 \qquad \text{at} \quad r = a, b, \\ &\textstyle\int_0^l \sigma_{r\theta}(r, \theta, z) \cos(\bar{\delta}_i z) \, \mathrm{d}z = 0 \qquad \text{at} \quad r = a, b. \end{aligned} \tag{18}$$

The displacement and stress fields are written in the series form with the indices i and j which are truncated with N_1 and N_2 terms respectively. Using Eqs. (18) and Appendix A the following linear algebraic system of equations $(N_1 + 4N_2) \times (N_1 + 4N_2)$ is obtained:

$$[\mathbf{M}_{\mathrm{st}}]_{5\times5} [\mathbf{\Delta}_{\mathrm{t}}]_{5\times1} = [\mathbf{0}]_{5\times1}. \tag{19}$$

The components of matrix and vectors in Eq. (19) are

$$\begin{aligned} &\mathbf{M}_{\mathrm{st}} = \left[M_{\mathrm{st},ij}\right]_{\tau\times\eta}, \tau = \begin{cases} N_1 \ \text{at} \ s = 1 \\ N_2 \ \text{at} \ s \neq 1 \end{cases}, \eta = \begin{cases} N_1 \ \text{at} \ t = 1, \\ N_2 \ \text{at} \ t \neq 1, \end{cases} \\ &\mathbf{\Delta}_1 = \left\{A_{1j}\right\}_{N_1\times1}, \mathbf{\Delta}_2 = \left\{A_{4j}\right\}_{N_2\times1}, \mathbf{\Delta}_3 = \left\{B_{4j}\right\}_{N_2\times1}, \mathbf{\Delta}_4 = \left\{A_{6j}\right\}_{N_2\times1}, \mathbf{\Delta}_5 = \left\{B_{6j}\right\}_{N_2\times1}, \end{aligned} \tag{20}$$

where the components of the matrix $\mathbf{M}_{st}$ are given in Appendix C. Setting the determinant value of $[\mathbf{M}_{st}]_{5\times5}$ equal to zero, the natural frequencies of the cylinder can be obtained.

2.2. Fixed-end hollow circular cylinder

In this case the combination of the displacement and stress boundary conditions are considered to show that the present method is capable to evaluate the other boundary conditions, and to show that the accuracy of the results is affected by the type of boundary conditions. The boundary conditions of the fixed-end hollow circular cylinder are defined as

$$\begin{aligned} &\sigma_{rr} = \sigma_{r\theta} = \sigma_{rz} = 0 \quad \text{at} \quad r = a, b, \\ &u_r = u_\theta = u_z = 0 \qquad \text{at} \quad z = -l, l. \end{aligned} \tag{21}$$

The following boundary conditions are exactly satisfied.

$$\begin{aligned} &\sigma_{rz} = 0 \qquad \text{at} \quad r = a, b, \\ &u_r = u_\theta = 0 \quad \text{at} \quad z = -l, l. \end{aligned} \tag{22}$$

And the five remaining boundary conditions are satisfied using the orthogonalization technique.

$$\begin{aligned} &\sigma_{rr} = \sigma_{r\theta} = 0 \quad \text{at} \quad r = a, b, \\ &u_z = 0 \qquad \text{at} \quad z = -l, l. \end{aligned} \tag{23}$$

For the first form of the solution ''symmetric mode'', the boundary conditions (22) are employed assuming:

$$\begin{aligned} &A_2 = A_1 \frac{\alpha\cos(\delta_1 l)}{\delta_2\cos(\delta_2 l)} \quad B_2 = B_1 \frac{\alpha\cos(\delta_1 l)}{\delta_2\cos(\delta_2 l)}, \\ &A_3 = -A_1 \frac{\cos(\delta_1 l)}{\cos(\delta_2 l)} \quad B_3 = -B_1 \frac{\cos(\delta_1 l)}{\cos(\delta_2 l)}, \\ &A_{5i} = K_{1i}A_{4i} + K_{2i}B_{4i} + K_{3i}A_{6i} + K_{4i}B_{6i}, \quad B_{6i} = \Lambda_{1i}A_{4i} + \Lambda_{2i}B_{4i} + \Lambda_{3i}A_{6i} + \Lambda_{4i}B_{6i}, \\ &\bar{\delta}_i = \frac{(2i-1)\pi}{2l}, \quad i = 1, 2, 3, \ldots, \end{aligned} \tag{24}$$

where K_{ki} and Λ_{ki} ($k = 1, 2, 3, 4$) are the same as those presented in Appendix B. The stresses boundary conditions in Eq. (23) are satisfied using orthogonalization technique similar to those presented in Eq. (18) and the displacement boundary condition in Eq. (23) is satisfied as follows:

$$\int_a^b u_z(r, \theta, l) P_n(\alpha_j r) r \, \mathrm{d}r = 0, \tag{25}$$

where $\alpha_j (j = 1,2,3, \ldots)$ is calculated in the same way as the case of free-end cylinder. Utilizing the equations which are obtained from the satisfaction of the boundary conditions in Eq. (23) leads to the linear algebraic system of equations similar to that obtained in Eq. (19). The components of the matrix $\mathbf{M}_{st}$ in Eq. (19) related to this case are given in Appendix D. In the following section the convergence, accuracy and numerical robustness of the present method are evaluated.

3. Results and discussions

The analysis developed in the preceding sections allows the investigation of the convergence, accuracy and robustness of the method for the explained boundary conditions.

3.1. Free-end hollow circular cylinder

The convergence of the method is evaluated for the two lowest frequencies of the symmetric and antisymmetric modes with circumferential wave number of 0 and 1. The results are presented in Figs. 2 and 3.

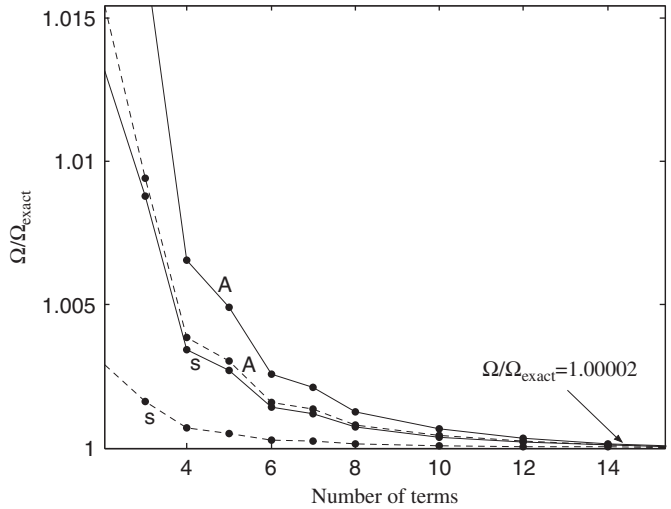

Fig. 2. Ratio of $\Omega/\Omega_{\text{exact}}$ versus the number of series terms for symmetric mode (S) and antisymmetric mode (A) with $H = 1$, $L = 2$ and $n = 0$ (- - -, first natural frequency; —, second natural frequency).

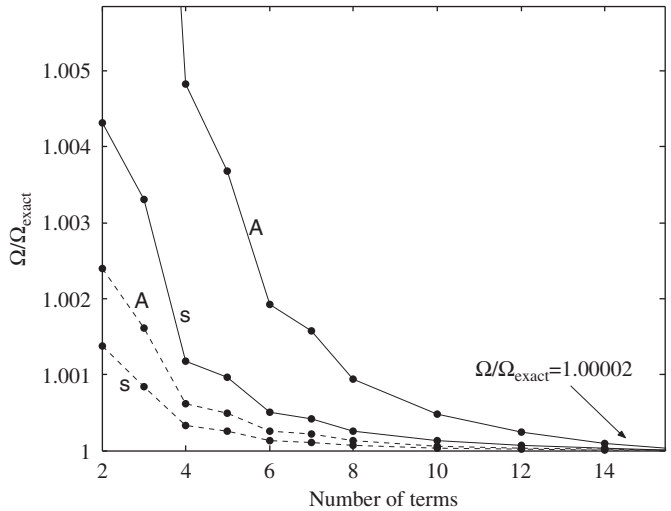

Fig. 3. Ratio of $\Omega/\Omega_{\text{exact}}$ versus the number of series terms for symmetric mode (S) and antisymmetric mode (A) with $H = 1$, $L = 2$ and $n = 1$ (- - -, first natural frequency; —, second natural frequency).

Ω is the non-dimensional natural frequency defined as

$$\Omega = \frac{\omega b}{C_2}, \tag{26}$$

where b is the outer radius and C_2 is the velocity of distortional wave (H is the ratio of the thickness with respect to the mean radius and L is the ratio of the length over the mean radius). The Poisson's ratio is taken as 0.3 in the present work. Ω is calculated from Eq. (26) and Ω_{exact} is the natural frequency obtained from the series with a tolerance convergence of 0.00001. In the case of $n = 0$, the rate of convergence is similar to that obtained by Hutchinson and El-Azhari [11]. In Table 1 the high precision results of the present method are compared with those obtained by So and Leissa [14] and Zhou et al. [19]. The results are presented for the first four natural frequencies of the circumferential wave number 0 with $H = 1.4$ and $L = 1$, 4 and 10. This table

Table 1
Comparison between the results of the present method with those obtained by So and Leissa [14] and Zhou et al. [19] for the free-end hollow cylinder with $H = 1.4$ and $n = 0$

L	Non-dimensional natural frequency (Ω)					
	Symmetric mode			Antisymmetric mode		
	Present	[14]	[19]	Present	[14]	[19]
1	3.0858	3.0858	3.0857	1.7887	1.7884	1.7883
	7.2376	7.2372	7.2374	5.3172	5.3168	5.3169
	7.7658	7.8200	7.8204	6.7195	6.7194	6.7195
	8.9148	8.9145	8.9148	9.6716	9.6715	9.6718
4	2.0239	2.0239	2.0239	2.7783	2.7783	2.7782
	2.8076	2.8076	2.8074	3.1772	3.1770	3.1769
	3.4970	3.4971	3.4969	4.5259	4.5259	4.5259
	4.2570	4.2568	4.2567	4.7387	4.7388	4.7386
10	0.8551	0.8551	0.8551	1.6646	1.6646	1.6646
	2.3271	2.3271	2.3270	2.7274	2.7275	2.7274
	2.7958	2.7953	2.7953	2.8252	2.8246	2.8245
	3.0917	3.0911	3.0911	3.3404	3.3407	3.3405

shows that the obtained results are in good agreement with those given by So and Leissa [14] in some cases and they are closer to the results obtained by Zhou et al. [19] in the other cases.

Since some of the boundary conditions are approximately satisfied such as those given in Eq. (13), the precision of the method is evaluated by the estimation of the natural frequencies which are presented in Table 1 and using the calculation of boundaries stresses. To evaluate the error percentage in the calculated boundaries stresses, the stresses satisfied by the orthogonalization technique on the boundaries for the first symmetric natural frequency are divided by the maximum value of the stresses on the normal cross-sections. The obtained error percentage for σ_{zz}, σ_{rr} and $\sigma_{r\theta}$ are calculated and depicted in Figs. 4, 5 and 6, respectively. Fig. 4 shows that the error percentage reduces as the number of terms in the series increases. In the case of σ_{zz}, increasing the number of terms from 15 to 35 in both series leads to a reduction in the minimum error percentage from 1.2% to less than 0.5%, while a noticeable decreasing in error percentage is not obtained next to the boundaries edges. Figs. 4 and 5 show that through the major part of the boundaries the error percentage is less than 1% for σ_{zz} and less than 0.4% for σ_{rr}. Fig. 6 shows that the error percentage for $\sigma_{r\theta}$ is less than 0.02% on the major part of the inner and outer boundaries. According to the results presented in Figs. 4–6, it is concluded that the boundary conditions satisfactions are obtained with an acceptable error percentage. It is noted that the error percentage at the boundaries' edges is higher in comparison with the rest of the boundaries.

The mode shapes of the first three natural frequencies are presented in Fig. 7 to illustrate the symmetric and antisymmetric mode shapes and the differences between them. The highly accurate first four natural frequencies are presented in Table 2 for three values of the $H = 0.2$, 1 and 1.8 and three values of the $L = 1$, 5 and 10.

3.2. Fixed-end hollow circular cylinder

In this section accuracy and convergence of the method are evaluated for a hollow circular cylinder with the fixed-end boundary conditions. Convergence is carried out for the lowest two frequencies of the symmetric and antisymmetric modes with circumferential wave number of 0 and 1 as illustrated in Table 3. The convergence of the method in this case is almost the same as that evaluated in the free-end hollow circular cylinder case. It is seen that using 15 terms in both series leads to the desirable precision in the results. The capability of the method to satisfy the boundary conditions is re-examined for the fixed-end boundary

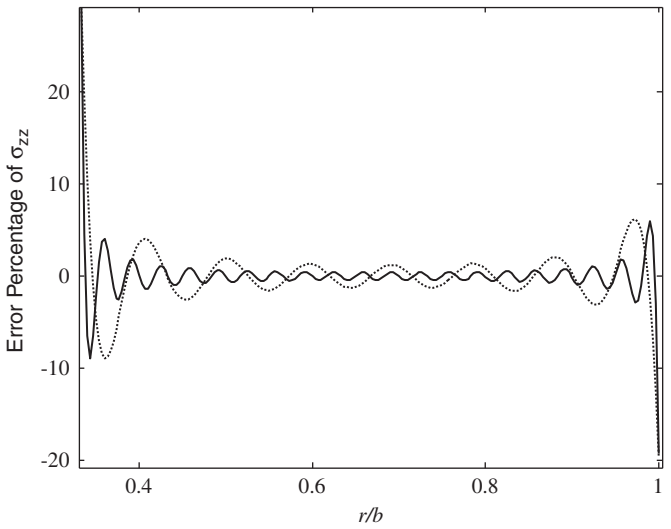

Fig. 4. The error percentage of σ_{zz} along the boundaries at $z = -l$ and l for $H = 1$, $L = 2$ and $n = 1$ in the free-end case (…, 15 terms in series; —, 35 terms in series).

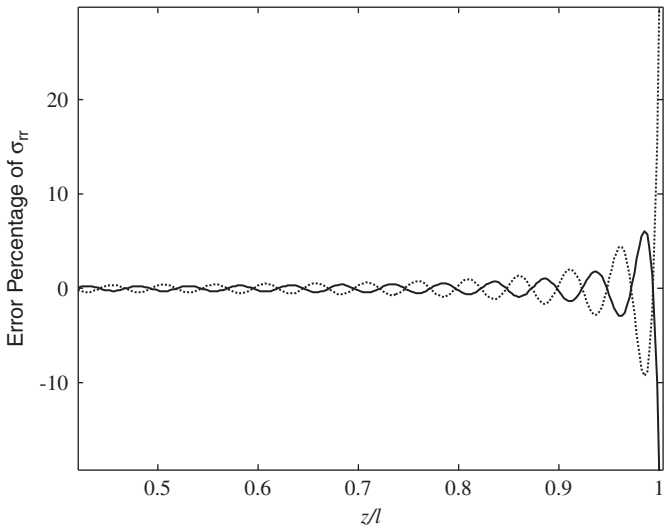

Fig. 5. The error percentage of σ_{rr} along the boundaries at $r = a$ and b for $H = 1$, $L = 2$ and $n = 1$ in the free-end case (…, r = inner radius; —, r = outer radius).

conditions using the evaluations of u_z, σ_{rr} and $\sigma_{r\theta}$. The error percentages are calculated similar to those explained in the former case except for u_z in which the z-displacements on the boundaries are divided by the maximum value of displacement on the normal cross-section. Fig. 8 shows that the error percentage for u_z decreases rapidly while the number of series terms increases to 35. For example in the case of u_z as the number of terms increases from 15 to 35 in both series, the minimum error percentage decreases from 0.05% to less than 0.005%. At the boundaries edges, the error percentage decreases from 0.8% to less than 0.4%. Fig. 9 shows that on the major part of the boundaries the error percentage is less than 0.3% for σ_{rr}. Clearly, similar to the case of free-end boundary conditions the error percentage for $\sigma_{r\theta}$ is almost zero

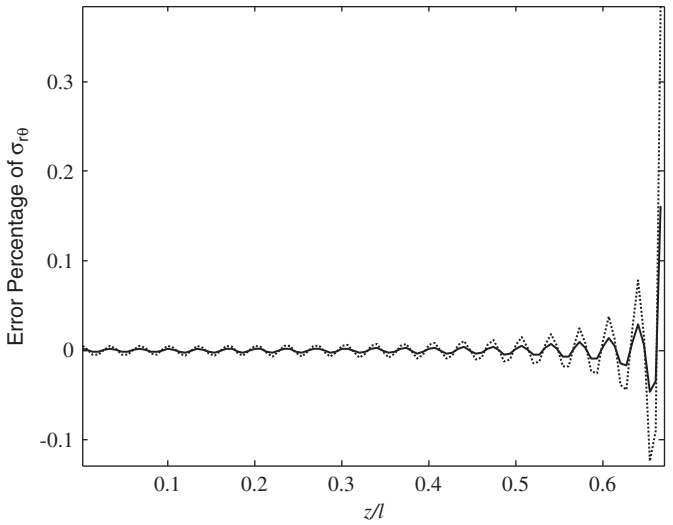

Fig. 6. The error percentage of $\sigma_{r\theta}$ along the boundaries at $r = a$ and b for $H = 1$, $L = 2$ and $n = 1$ in the free-end case (…, r = inner radius; — r = outer radius).

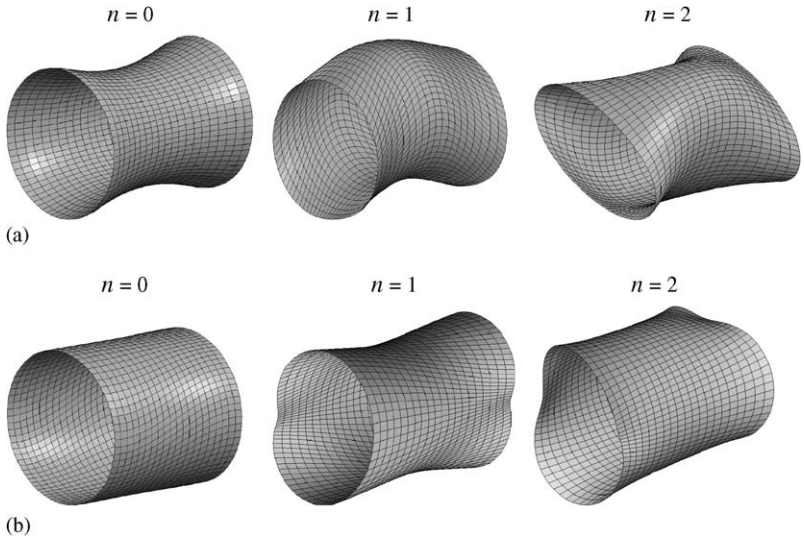

Fig. 7. The free-end cylinder mode shapes of the first natural frequencies for $n = 0$, 1 and 2, (a) symmetric mode (b) antisymmetric mode.

over the most of the boundaries as shown in Fig. 10. It can be concluded that the boundary conditions for a fixed-end cylinder are satisfied better than those for a free-end cylinder. To verify the present semi-analytical method in the case of fixed-end boundary conditions, the non-dimensional natural frequencies corresponding to the mode shapes presented in Fig. 11 are compared with those provided by Zhou et al. [19] in Table 4. It is noted that in both cases of, "symmetric" and "antisymmetric" modes, there are excellent agreements between the natural frequencies obtained using the present method with those given by the Ritz–Chebyshev method [19]. Moreover, it may be noticed that, increasing the ratio of the length over the mean radius leads to the decreasing in the natural frequencies. Generally, the results obtained for a fixed-end cylinder using the present method are in better agreement with those reported in the literatures than those obtained for a free-end cylinder. It is considered because low-order Bessel functions

Table 2
The first four natural frequencies of the free-end hollow circular cylinders with three values of H and L, for $n = 0$, 1 and 2

H	L	Non-dimensional natural frequency (Ω)					
		$n = 0$		$n = 1$		$n = 2$	
		Sym[a]	Ant[b]	Sym[a]	Ant[b]	Sym[a]	Ant[b]
		1.7726	1.7447	2.4706	1.6514	0.2740	0.4467
	1	2.6832	5.1756	2.7435	4.0280	2.9186	2.0080
		5.8555	11.5393	5.6706	5.2441	3.8021	5.1297
		8.3328	11.6279	7.3440	10.2811	5.6079	5.4663
		1.0855	1.6827	0.6715	0.9949	0.2807	0.3016
		1.7574	1.7746	1.4027	1.3223	0.4793	0.8232
0.2	5	1.8215	1.9115	1.6063	1.7685	1.2038	1.5684
		1.9162	2.3472	2.0241	2.0721	1.9337	2.1105
		0.5545	1.0855	0.2317	0.4905	0.2817	0.2841
		1.5068	1.6830	0.7547	0.9664	0.3164	0.4007
	10	1.7372	1.7614	1.1496	1.1630	0.5412	0.7139
		1.8331	1.7966	1.3326	1.3229	0.8998	1.0882
		2.6092	1.8191	2.8248	2.4417	1.4272	1.0899
		6.6422	6.1879	6.2329	5.2108	4.0573	3.8487
	1	7.0580	7.0129	6.7939	5.9905	6.5273	6.0666
		8.2698	9.8304	7.3249	6.9858	6.9941	6.2521
		1.4753	2.3874	1.0117	1.4856	1.4522	1.4479
1		2.4682	2.5699	2.1341	2.1347	1.6396	2.1406
	5	2.8273	3.4615	2.8511	2.7819	2.7965	2.9982
		3.0655	3.7091	2.9620	3.2916	3.4906	3.6202
		0.7554	1.4753	0.3470	0.7434	1.4536	1.4523
	10	2.0648	2.3562	1.1676	1.4818	1.7678	1.5754
		2.4824	2.5123	1.7632	1.7582	2.3634	2.0387
		2.6688	2.8271	2.1850	2.1392	2.9619	2.6946
		3.3826	1.7459	2.7329	3.1038	2.3081	1.1037
		7.8785	4.8152	5.8052	5.8001	4.1923	4.4069
	1	8.7639	7.8746	6.8054	6.4918	7.0816	6.6371
		9.9487	8.9141	8.7743	6.8765	8.1876	7.3547
		1.8464	2.9192	1.4070	1.8872	2.2032	2.0531
		2.9197	3.0698	2.6697	2.8129	2.3177	2.8377
		3.6819	4.2363	2.9822	3.1516	3.5923	3.5464
1.8	5	4.1861	4.5017	3.5529	3.9416	4.3064	4.2776
		0.9543	1.8465	0.5029	1.0424	2.2334	2.1217
		2.5519	2.9195	1.6032	1.8839	2.3117	2.3140
	10	2.9369	3.0336	2.2334	2.3055	2.5085	2.8311
		3.3981	3.6313	2.7677	2.7540	3.1903	3.1998

[a]Symmetric mode.
[b]Antisymmetric mode.

are employed in the displacements components related to the end boundary conditions for a fixed-end cylinder.

4. Conclusion

A general solution using the technique of variables separation on the basis of linear 3D theory of elasticity with the minimum required coefficients is developed to analyze the vibration of finite circular cylinders. The

Table 3
Convergence of the method in the case of fixed-end cylinder for $H = 2/3$ and $L = 4$ with equal number of terms in both of series

Number of terms	Non-dimensional natural frequency (Ω)							
	$n = 0$				$n = 1$			
	Symmetric mode		Antisymmetric mode		Symmetric mode		Antisymmetric mode	
	Ω_1	Ω_2	Ω_1	Ω_2	Ω_1	Ω_2	Ω_1	Ω_2
2	2.31685	2.87882	1.71649	2.61639	0.81449	2.52369	1.61305	2.14522
3	2.31385	2.86753	1.70361	2.56643	0.81349	2.52927	1.60685	2.13406
4	2.31308	2.87672	1.69997	2.56324	0.81522	2.52736	1.60993	2.13254
5	2.31280	2.87664	1.69796	2.56179	0.81516	2.52732	1.60975	2.13137
6	2.31264	2.87867	1.69701	2.56155	0.81549	2.52912	1.61051	2.13092
7	2.31257	2.87867	1.69642	2.56128	0.81546	2.52913	1.61049	2.13056
8	2.31251	2.87938	1.69606	2.56121	0.81556	2.52978	1.61076	2.13037
9	2.31248	2.87935	1.69582	2.56109	0.81553	2.52977	1.61075	2.13022
10	2.31245	2.87966	1.69564	2.56106	0.81557	2.53006	1.61087	2.13013
11	2.31243	2.87962	1.69553	2.56099	0.81555	2.53005	1.61085	2.13005
12	2.31241	2.87978	1.69543	2.56097	0.81557	2.53021	1.61091	2.12999
13	2.31240	2.87975	1.69536	2.56093	0.81555	2.53019	1.61089	2.12995
14	2.31239	2.87984	1.69529	2.56091	0.81555	2.53028	1.61093	2.12991
15	2.31238	2.87981	1.69525	2.56088	0.81554	2.53027	1.61092	2.12988
16	2.31237	2.87986	1.69521	2.56087	0.81554	2.53033	1.61093	2.12985

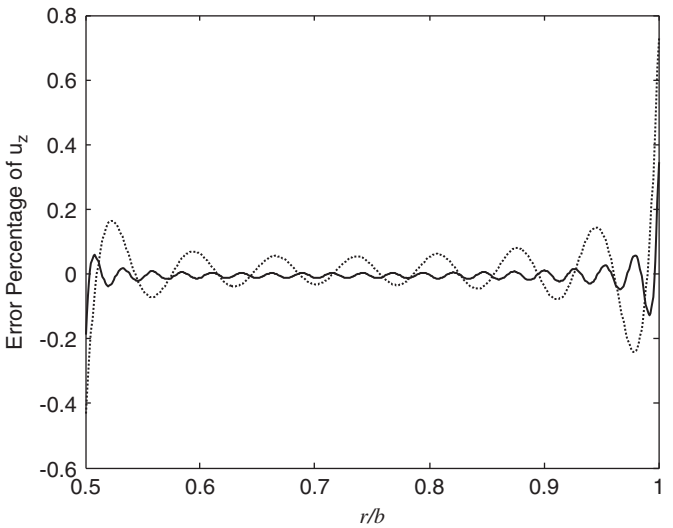

Fig. 8. The error percentage of u_z along the boundaries at $z = -l$ and l for $H = 1$, $L = 2$ and $n = 1$ in the fixed-end case (…, 15 terms in series; —, 35 terms in series).

vibration of finite circular cylinders with the free-end and the fixed-end boundary conditions are evaluated by the present method. Although the entire boundary conditions cannot be exactly satisfied and using the orthogonalization technique leads to the acceptable results. To evaluate the precision of the present method the natural frequencies are calculated for different geometries and compared with those reported in the pervious studies. The results are in good agreement with the reported results in the literatures. Satisfactory

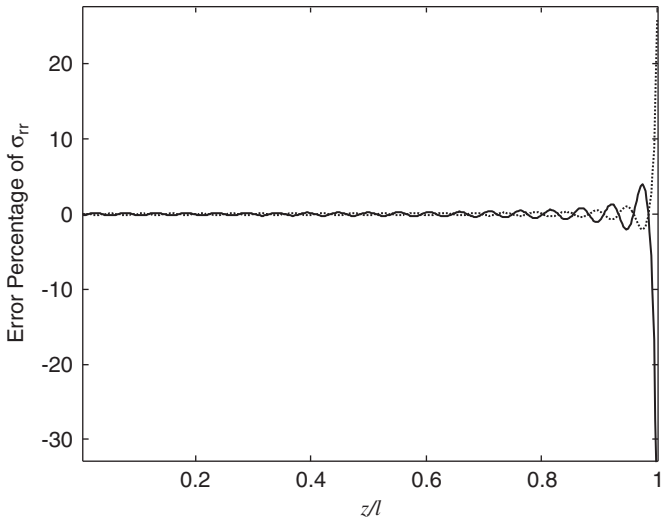

Fig. 9. The error percentage of σ_{rr} along the boundaries at $r = a$ and b for $H = 1$, $L = 2$ and $n = 1$ in the fixed-end case (…, r = inner radius; — r = outer radius).

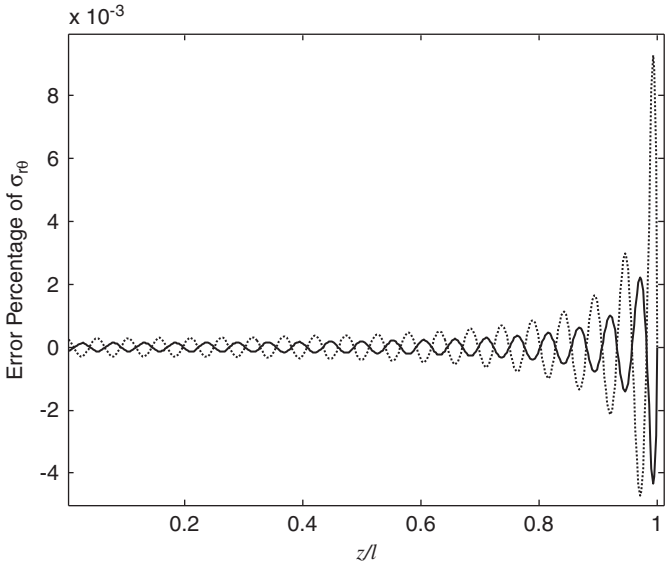

Fig. 10. The error percentage of $\sigma_{r\theta}$ along the boundaries at $r = a$ and b for $H = 1$, $L = 2$ and $n = 1$ in the fixed-end case (…, r = inner radius; —, r = outer radius).

convergence is also obtained with only a moderate number of terms in both series. It is shown that, the obtained errors of the approximately satisfied boundary conditions for the fixed-end case are less than those obtained for the free-end case. It may be because low-order Bessel functions are used in the displacement components related to the end boundary conditions for the fixed-end cylinder. The advantages of the proposed approach are its generality, accuracy and good convergence of the solution with a relatively small-sized coefficient matrix.

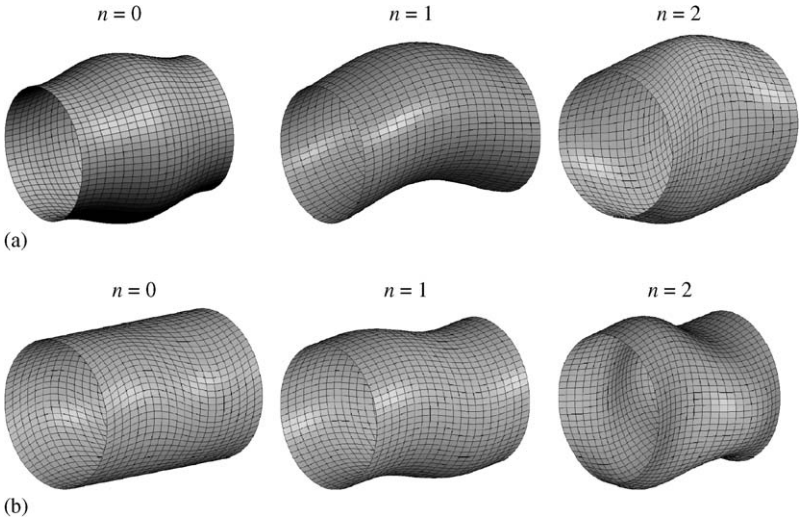

Fig. 11. The fixed-end cylinder mode shapes of the first natural frequencies for $n = 0$, 1 and 2, (a) symmetric mode (b) antisymmetric mode.

Table 4
Comparison between the results of the present method with those obtained by Zhou et al. [19] for the fixed-end hollow cylinder with $H = 2/3$.

L	n	Non-dimensional natural frequency (Ω)			
		Symmetric mode		Antisymmetric mode	
		Present	[19]	Present	[19]
4	0	2.3123	2.3123	1.6949	1.6949
		2.8798	2.8798	2.5607	2.5607
		3.6515	3.6514	3.5883	3.5883
		4.4161	4.4161	5.2166	5.2166
	1	0.8155	0.8155	1.6109	1.6109
		2.5304	2.5304	2.1297	2.1297
		2.8947	2.8947	3.3630	3.3630
		3.4641	3.4640	3.4760	3.4760
	2	1.2396	1.2396	1.8288	1.8288
		2.6408	2.6409	3.0645	3.0645
		3.7995	3.7995	3.5644	3.5645
		4.5121	4.5121	4.4681	4.4679
8	0	1.6432	1.6432	0.8509	0.8508
		2.2846	2.2847	2.0944	2.1214
		2.4041	2.4041	2.3953	2.3954
		2.5794	2.5794	2.7290	2.7288
	1	0.3395	0.3395	0.7053	0.7054
		1.3338	1.1338	1.5343	1.5343
		1.9880	1.9880	1.6318	1.6318
		2.0930	2.0930	2.4485	2.4485
	2	1.0288	1.0288	1.1746	1.1747
		1.4285	1.4286	1.7648	1.7648
		2.1562	2.1562	2.5796	2.5797
		2.9909	2.9908	2.7846	2.7846

Appendix A

The stress components of symmetric and antisymmetric modes are as

$$\begin{aligned}\sigma_{rr} = 2\mu\Bigg\{&\Bigg[A_1\left(\left(\frac{n(n-1)}{r^2}+\delta_1^2-\frac{(\alpha^2+\delta_2^2)}{2}\right)J_n(\alpha r)+\frac{\alpha}{r}J_{n+1}(\alpha r)\right)\\&+B_1\left(\left(\frac{n(n-1)}{r^2}+\delta_1^2-\frac{(\alpha^2+\delta_2^2)}{2}\right)Y_n(\alpha r)+\frac{\alpha}{r}Y_{n+1}(\alpha r)\right)\Bigg]\begin{Bmatrix}\cos(\delta_1 z)\\ \sin(\delta_1 z)\end{Bmatrix}\\&+\Bigg[A_2\delta_2\left(\alpha J_n(\alpha r)-\frac{(n+1)}{r}J_{n+1}(\alpha r)\right)+B_2\delta_2\left(\alpha Y_n(\alpha r)-\frac{(n+1)}{r}Y_{n+1}(\alpha r)\right)\\&+\left\{A_3\frac{n}{r}\left(\frac{(n-1)}{r}J_n(\alpha r)-\alpha J_{n+1}(\alpha r)\right)+B_3\frac{n}{r}\left(\frac{(n-1)}{r}Y_n(\alpha r)-\alpha Y_{n+1}(\alpha r)\right)\right\}\begin{Bmatrix}1\\-1\end{Bmatrix}\Bigg]\begin{Bmatrix}\cos(\delta_2 z)\\ \sin(\delta_2 z)\end{Bmatrix}\\&+\Bigg[A_4\left(\left(\frac{n(n-1)}{r^2}+\frac{\bar{\delta}^2-\bar{\alpha}_2^2}{2}\right)J_n(\bar{\alpha}_1 r)+\frac{\bar{\alpha}_1}{r}J_{n+1}(\bar{\alpha}_1 r)\right)\\&+B_4\left(\left(\frac{n(n-1)}{r^2}+\frac{\bar{\delta}^2-\bar{\alpha}_2^2}{2}\right)Y_n(\bar{\alpha}_1 r)+\frac{\bar{\alpha}_1}{r}Y_{n+1}(\bar{\alpha}_1 r)\right)+A_5\bar{\delta}\left(\bar{\alpha}_2 J_n(\bar{\alpha}_2 r)-\frac{(n+1)}{r}J_{n+1}(\bar{\alpha}_2 r)\right)\\&+B_5\bar{\delta}\left(\bar{\alpha}_2 Y_n(\bar{\alpha}_2 r)-\frac{(n+1)}{r}Y_{n+1}(\bar{\alpha}_2 r)\right)+\left\{A_6\frac{n}{r}\left(\frac{(n-1)}{r}J_n(\bar{\alpha}_2 r)-\bar{\alpha}_2 J_{n+1}(\bar{\alpha}_2 r)\right)\right.\\&\left.+B_6\frac{n}{r}\left(\frac{(n-1)}{r}Y_n(\bar{\alpha}_2 r)-\bar{\alpha}_2 Y_{n+1}(\bar{\alpha}_2 r)\right)\right\}\begin{Bmatrix}1\\-1\end{Bmatrix}\Bigg]\begin{Bmatrix}\cos(\bar{\delta}z)\\ \sin(\bar{\delta}z)\end{Bmatrix}\Bigg\}\begin{Bmatrix}\cos(n\theta)\\ \sin(n\theta)\end{Bmatrix}e^{i\omega t},\end{aligned}\tag{A.1}$$

$$\begin{aligned}\sigma_{r\theta} = \mu\Bigg\{&\Bigg[A_1\frac{2n}{r}\left(\frac{(1-n)}{r}J_n(\alpha r)+\alpha J_{n+1}(\alpha r)\right)\\&+B_1\frac{2n}{r}\left(\frac{(1-n)}{r}Y_n(\alpha r)+\alpha Y_{n+1}(\alpha r)\right)\Bigg]\begin{Bmatrix}1\\-1\end{Bmatrix}\begin{Bmatrix}\cos(\delta_1 z)\\ \sin(\delta_1 z)\end{Bmatrix}\\&+\Bigg[\left\{A_2\delta_2\left(\alpha J_n(\alpha r)-\frac{2(n+1)}{r}J_{n+1}(\alpha r)\right)+B_2\delta_2\left(\alpha Y_n(\alpha r)-\frac{2(n+1)}{r}Y_{n+1}(\alpha r)\right)\right\}\begin{Bmatrix}1\\-1\end{Bmatrix}\\&+A_3\left(\left(\alpha^2-\frac{2n(n-1)}{r^2}\right)J_n(\alpha r)-\frac{2\alpha}{r}J_{n+1}(\alpha r)\right)+B_3\left(\left(\alpha^2-\frac{2n(n-1)}{r^2}\right)Y_n(\alpha r)-\frac{2\alpha}{r}Y_{n+1}(\alpha r)\right)\Bigg]\begin{Bmatrix}\cos(\delta_2 z)\\ \sin(\delta_2 z)\end{Bmatrix}\\&+\Bigg[\left\{A_4\frac{2n}{r}\left(\frac{(1-n)}{r}J_n(\bar{\alpha}_1 r)+\bar{\alpha}_1 J_{n+1}(\bar{\alpha}_1 r)\right)+B_4\frac{2n}{r}\left(\frac{(1-n)}{r}Y_n(\bar{\alpha}_1 r)+\bar{\alpha}_1 Y_{n+1}(\bar{\alpha}_1 r)\right)\right.\\&\left.+A_5\bar{\delta}\left(\bar{\alpha}_2 J_n(\bar{\alpha}_2 r)-\frac{2(n+1)}{r}J_{n+1}(\bar{\alpha}_2 r)\right)+B_5\bar{\delta}\left(\bar{\alpha}_2 Y_n(\bar{\alpha}_2 r)-\frac{2(n+1)}{r}Y_{n+1}(\bar{\alpha}_2 r)\right)\right\}\begin{Bmatrix}1\\-1\end{Bmatrix}\\&+A_6\left(\left(\bar{\alpha}_2^2-\frac{2n(n-1)}{r^2}\right)J_n(\bar{\alpha}_2 r)-\frac{2\bar{\alpha}_2}{r}J_{n+1}(\bar{\alpha}_2 r)\right)\\&+B_6\left(\left(\bar{\alpha}_2^2-\frac{2n(n-1)}{r^2}\right)Y_n(\bar{\alpha}_2 r)-\frac{2\bar{\alpha}_2}{r}Y_{n+1}(\bar{\alpha}_2 r)\right)\Bigg]\begin{Bmatrix}\cos(\bar{\delta}z)\\ \sin(\bar{\delta}z)\end{Bmatrix}\Bigg\}\begin{Bmatrix}\sin(n\theta)\\ \cos(n\theta)\end{Bmatrix}e^{i\omega t},\end{aligned}\tag{A.2}$$

$$\begin{aligned}\sigma_{rz} = \mu\Bigg\{&\Bigg[\left\{2A_1\delta_1\left(-\frac{n}{r}J_n(\alpha r)+\alpha J_{n+1}(\alpha r)\right)+2B_1\delta_1\left(-\frac{n}{r}Y_n(\alpha r)+\delta Y_{n+1}(\alpha r)\right)\right\}\begin{Bmatrix}1\\-1\end{Bmatrix}\Bigg]\begin{Bmatrix}\sin(\delta_1 z)\\ \cos(\delta_1 z)\end{Bmatrix}\\&+\Bigg[\left\{A_2\left(-\frac{n\alpha}{r}J_n(\alpha r)+(\alpha^2-\delta_2^2)J_{n+1}(\alpha r)\right)+B_2\left(-\frac{n\alpha}{r}Y_n(\alpha r)+(\alpha^2-\delta_2^2)Y_{n+1}(\alpha r)\right)\right\}\begin{Bmatrix}1\\-1\end{Bmatrix}\end{aligned}$$

$$
\begin{aligned}
&- A_3\frac{n\delta_2}{r}J_n(\alpha r) - B_3\frac{n\delta_2}{r}Y_n(\alpha r)\Big]\begin{Bmatrix}\sin(\delta_2 z)\\ \cos(\delta_2 z)\end{Bmatrix} + \Big[\Big\{2A_4\bar{\delta}\Big(-\frac{n}{r}J_n(\bar{\alpha}_1 r) + \bar{\alpha}_1 J_{n+1}(\bar{\alpha}_1 r)\Big)\\
&+2B_4\bar{\delta}\Big(\frac{n}{r}Y_n(\bar{\alpha}_1 r) - \bar{\alpha}_1 Y_{n+1}(\bar{\alpha}_1 r)\Big) + A_5\Big(-\frac{n\bar{\alpha}_2}{r}J_n(\bar{\alpha}_2 r) + (\bar{\alpha}_2^2 - \bar{\delta}^2)J_{n+1}(\bar{\alpha}_2 r)\Big)\\
&+B_5\Big(-\frac{n\bar{\alpha}_2}{r}Y_n(\bar{\alpha}_2 r) + (\bar{\alpha}_2^2 - \bar{\delta}^2)Y_{n+1}(\bar{\alpha}_2 r)\Big)\Big\}\begin{Bmatrix}1\\ -1\end{Bmatrix} - A_6\frac{n\bar{\delta}}{r}J_n(\bar{\alpha}_2 r)\\
&-B_6\frac{n\bar{\delta}}{r}Y_n(\bar{\alpha}_2 r)\Big]\begin{Bmatrix}\sin(\bar{\delta}z)\\ \cos(\bar{\delta}z)\end{Bmatrix}\Big\}\begin{Bmatrix}\cos(n\theta)\\ \sin(n\theta)\end{Bmatrix}e^{i\omega t},
\end{aligned}
\tag{A.3}
$$

$$
\begin{aligned}
\sigma_{\theta z} = \mu\Big\{&\frac{2n\delta_1}{r}(A_1 J_n(\alpha r) + B_1 Y_n(\alpha r))\begin{Bmatrix}\sin(\delta_1 z)\\ \cos(\delta_1 z)\end{Bmatrix}\\
&+\Big[A_2\Big(\frac{n\alpha}{r}J_n(\alpha r) - \delta_2^2 J_{n+1}(\alpha r)\Big) + B_2\Big(\frac{n\alpha}{r}Y_n(\alpha r) - \delta_2^2 Y_{n+1}(\alpha r)\Big)\\
&+\Big\{A_3\delta_2\Big(\frac{n}{r}J_n(\alpha r) - \alpha J_{n+1}(\alpha r)\Big) + B_3\delta_2\Big(\frac{n}{r}Y_n(\alpha r) - \alpha Y_{n+1}(\alpha r)\Big)\Big\}\begin{Bmatrix}1\\ -1\end{Bmatrix}\Big]\begin{Bmatrix}\sin(\delta_2 z)\\ \cos(\delta_2 z)\end{Bmatrix}\\
&+\Big[\frac{2n\bar{\delta}}{r}(A_4 J_n(\bar{\alpha}_1 r) + B_4 Y_n(\bar{\alpha}_1 r)) + A_5\Big(\frac{n\bar{\alpha}_2}{r}J_n(\bar{\alpha}_2 r) - \bar{\delta}^2 J_{n+1}(\bar{\alpha}_2 r)\Big)\\
&+B_5\Big(\frac{n\bar{\alpha}_2}{r}Y_n(\bar{\alpha}_2 r) - \bar{\delta}^2 Y_{n+1}(\bar{\alpha}_2 r)\Big) + \Big\{A_6\bar{\delta}\Big(\frac{n}{r}J_n(\bar{\alpha}_2 r) - \bar{\alpha}_2 J_{n+1}(\bar{\alpha}_2 r)\Big)\\
&+B_6\bar{\delta}\Big(\frac{n}{r}Y_n(\bar{\alpha}_2 r) - \bar{\alpha}_2 Y_{n+1}(\bar{\alpha}_2 r)\Big)\Big\}\begin{Bmatrix}1\\ -1\end{Bmatrix}\Big]\begin{Bmatrix}\sin(\bar{\delta}z)\\ \cos(\bar{\delta}z)\end{Bmatrix}\Big\}\begin{Bmatrix}\sin(n\theta)\\ \cos(n\theta)\end{Bmatrix}e^{i\omega t}
\end{aligned}
\tag{A.4}
$$

$$
\begin{aligned}
\sigma_{zz} = 2\mu\Big\{&\frac{(\alpha^2 - \delta_2^2)}{2}(A_1 J_n(\alpha r) + B_1 Y_n(\alpha r))\begin{Bmatrix}\cos(\delta_1 z)\\ \sin(\delta_1 z)\end{Bmatrix}\\
&- \alpha\delta_2(A_2 J_n(\alpha r) + B_2 Y_n(\alpha r))\begin{Bmatrix}\cos(\delta_2 z)\\ \sin(\delta_2 z)\end{Bmatrix} + \Big[\Big(\bar{\alpha}_1^2 - \frac{\bar{\delta}^2 + \bar{\alpha}_2^2}{2}\Big)(A_4 J_n(\bar{\alpha}_1 r) + B_4 Y_n(\bar{\alpha}_1 r))\\
&- \bar{\alpha}_2\bar{\delta}(A_5 J_n(\bar{\alpha}_2 r) + B_5 Y_n(\bar{\alpha}_2 r))\Big]\begin{Bmatrix}\cos(\bar{\delta}z)\\ \sin(\bar{\delta}z)\end{Bmatrix}\Big\}\begin{Bmatrix}\cos(n\theta)\\ \sin(n\theta)\end{Bmatrix}e^{i\omega t}.
\end{aligned}
\tag{A.5}
$$

Appendix B

The coefficients K_{ki} and Λ_{-ki} ($k = 1,2,3,4,5$) of the expression of A_{5i} and B_{5i} versus A_{4i}, B_{4i}, A_{6i}, B_{6i} as

$$K_{1i} = (\Gamma_{1i}(a)\Psi_{2i}(b) - \Gamma_{1i}(b)\Psi_{2i}(a))/(\Psi_{2i}(a)\Gamma_{2i}(b) - \Gamma_{2i}(a)\Psi_{2i}(b)), \tag{B.1}$$

$$K_{2i} = (\Psi_{1i}(a)\Psi_{2i}(b) - \Psi_{1i}(b)\Psi_{2i}(a))/(\Psi_{2i}(a)\Gamma_{2i}(b) - \Gamma_{2i}(a)\Psi_{2i}(b)), \tag{B.2}$$

$$K_{3i} = (\Gamma_{3i}(a)\Psi_{2i}(b) - \Gamma_{3i}(b)\Psi_{2i}(a))/(\Psi_{2i}(a)\Gamma_{2i}(b) - \Gamma_{2i}(a)\Psi_{2i}(b)), \tag{B.3}$$

$$K_{4i} = (\Psi_{3i}(a)\Psi_{2i}(b) - \Psi_{3i}(b)\Psi_{2i}(a))/(\Psi_{2i}(a)\Gamma_{2i}(b) - \Gamma_{2i}(a)\Psi_{2i}(b)), \tag{B.4}$$

$$\Lambda_{1i} = (\Gamma_{1i}(a)\Gamma_{2i}(b) + \Gamma_{1i}(b)\Gamma_{2i}(a))/(\Psi_{2i}(a)\Gamma_{2i}(b) - \Gamma_{2i}(a)\Psi_{2i}(b)), \tag{B.5}$$

$$\Lambda_{2i} = (\Psi_{1i}(a)\Gamma_{2i}(b) + \Psi_{1i}(b)\Gamma_{2i}(a))/(\Psi_{2i}(a)\Gamma_{2i}(b) - \Gamma_{2i}(a)\Psi_{2i}(b)), \tag{B.6}$$

$$\Lambda_{3i} = (\Gamma_{3i}(a)\Gamma_{2i}(b) + \Gamma_{3i}(b)\Gamma_{2i}(a))/(\Psi_{2i}(a)\Gamma_{2i}(b) - \Gamma_{2i}(a)\Psi_{2i}(b)), \tag{B.7}$$

$$\Lambda_{4i} = (\Psi_{3i}(a)\Gamma_{2i}(b) + \Psi_{3i}(b)\Gamma_{2i}(a))/(\Psi_{2i}(a)\Gamma_{2i}(b) - \Gamma_{2i}(a)\Psi_{2i}(b)), \tag{B.8}$$

where

$$\begin{aligned}
\Gamma_{1i}(r) &= 2\bar{\delta}_i\left(-\frac{n}{r}J_n(\bar{\alpha}_{1i}r) + \bar{\alpha}_{1i}J_{n+1}(\bar{\alpha}_{1i}r)\right),\\
\Psi_{1i}(r) &= 2\bar{\delta}_i\left(-\frac{n}{r}Y_n(\bar{\alpha}_{1i}r) + \bar{\alpha}_{1i}Y_{n+1}(\bar{\alpha}_{1i}r)\right),\\
\Gamma_{2i}(r) &= -\left(\frac{n\bar{\alpha}_{2i}}{r}J_n(\bar{\alpha}_{2i}r) + \left(\bar{\delta}_i^2 - \bar{\alpha}_{2i}^2\right)J_{n+1}(\bar{\alpha}_{2i}r)\right),\\
\Psi_{2i}(r) &= -\left(\frac{n\bar{\alpha}_{2i}}{r}Y_n(\bar{\alpha}_{2i}r) + \left(\bar{\delta}_i^2 - \bar{\alpha}_{2i}^2\right)Y_{n+1}(\bar{\alpha}_{2i}r)\right),\\
\Gamma_{3i}(r) &= -\frac{n\bar{\delta}_i}{r}J_n(\bar{\alpha}_{2i}r),\\
\Psi_{3i}(r) &= -\frac{n\bar{\delta}_i}{r}Y_n(\bar{\alpha}_{2i}r)
\end{aligned} \tag{B.9}$$

and

$$\begin{aligned}
\bar{\delta}_i^2 + \bar{\alpha}_{1i}^2 &= \left(\frac{\omega_i^2}{C_1^2}\right),\\
\bar{\delta}_i^2 + \bar{\alpha}_{2i}^2 &= \left(\frac{\omega_i^2}{C_2^2}\right).
\end{aligned} \tag{B.10}$$

Appendix C

The components of M_{st} for the first form solution of the Free-end circular cylinder:

$$\begin{aligned}
M_{11,ij} = &\left[\frac{(\alpha_j^2 - \delta_{2j}^2)^2}{2}\cos(\delta_{1j}l) + 2\delta_{1j}\delta_{2j}\alpha_j^2\sin(\delta_{1j}l)\cot(\delta_{2j}l)\right], \quad i = 1,2,3...N_2,\\
&\times\frac{1}{2}\left[(b^2 - a^2) + \frac{n^2(P_n^2(\alpha_j a) - P_n^2(\alpha_j b))}{\alpha_j^2}\right], \qquad j = 1,2,3...N_1,
\end{aligned} \tag{C.1}$$

$$M_{12,ij} = \sum_{i=1}^{N_2}(-1)^{i-1}\left[\left(\bar{\alpha}_{1i}^2 - \frac{\bar{\delta}_i^2 + \bar{\alpha}_{2i}^2}{2}\right)\Pi_J(\alpha_j,\bar{\alpha}_{1i}) - K_{1i}\bar{\alpha}_{2i}\bar{\delta}_i\Pi_J(\alpha_j,\bar{\alpha}_{2i}) - \Lambda_{1i}\bar{\alpha}_{2i}\bar{\delta}_i\Pi_Y(\alpha_j,\bar{\alpha}_{2i})\right], \tag{C.2}$$

$$M_{13,ij} = \sum_{i=1}^{N_2}(-1)^{i-1}\left[\left(\bar{\alpha}_{1i}^2 - \frac{\bar{\delta}_i^2 + \bar{\alpha}_{2i}^2}{2}\right)\Pi_Y(\alpha_j,\bar{\alpha}_{1i}) - K_{2i}\bar{\alpha}_{2i}\bar{\delta}_i\Pi_J(\alpha_j,\bar{\alpha}_{2i}) - \Lambda_{2i}\bar{\alpha}_{2i}\bar{\delta}_i\Pi_Y(\alpha_j,\bar{\alpha}_{2i})\right], \tag{C.3}$$

$$M_{14,ij} = \sum_{i=1}^{N_2}(-1)^{i-1}\left[-K_{3i}\bar{\alpha}_{2i}\bar{\delta}_i\Pi_J(\alpha_j,\bar{\alpha}_{2i}) - \Lambda_{3i}\bar{\alpha}_{2i}\bar{\delta}_i\Pi_Y(\alpha_j,\bar{\alpha}_{2i})\right], \tag{C.4}$$

$$M_{15,ij} = \sum_{i=1}^{N_2}(-1)^{i-1}\left[-K_{4i}\bar{\alpha}_{2i}\bar{\delta}_i\Pi_J(\alpha_j,\bar{\alpha}_{2i}) - \Lambda_{4i}\bar{\alpha}_{2i}\bar{\delta}_i\Pi_Y(\alpha_j,\bar{\alpha}_{2i})\right], \tag{C.5}$$

where

$$\Pi_J(\alpha,\beta)=\beta\left(\frac{bJ'_n(\beta b)P_n(\alpha b)-aJ'_n(\beta a)P_n(\alpha a)}{\alpha^2-\beta^2}\right),$$
$$\Pi_Y(\alpha,\beta)=\beta\left(\frac{bY'_n(\beta b)P_n(\alpha b)-aY'(\beta a)P_n(\alpha a)}{\alpha^2-\beta^2}\right), \tag{C.6}$$

$$M_{21,ij}=\sum_{j=1}^{N_1}\left[(\alpha_j^2-\delta_{2j}^2)\left(\left(\frac{n(n-1)}{a^2}+\delta_{1j}^2-\frac{\alpha_j^2+\delta_{2j}^2}{2}\right)P_n(\alpha_j a)+\frac{\alpha_j}{a}Q_n(\alpha_j a)\right)\right.$$
$$\times\left(\frac{\sin((\bar\delta_i-\delta_{1j})l)}{2(\bar\delta_i-\delta_{1j})}+\frac{\sin((\bar\delta_i+\delta_{1j})l)}{2(\bar\delta_i+\delta_{1j})}\right)+2\delta_{1j}\delta_{2j}\frac{\sin(\delta_{1j}l)}{\sin(\delta_{2j}l)}\left(\left(\frac{n(n-1)}{a^2}-\alpha_j^2\right)P_n(\alpha_j a)\right.$$
$$\left.\left.+\frac{\alpha_j}{a}Q_n(\alpha_j a)\right)\times\left(\frac{\sin((\bar\delta_i-\delta_{2j})l)}{2(\bar\delta_i-\delta_{2j})}+\frac{\sin((\bar\delta_i+\delta_{2j})l)}{2(\bar\delta_i+\delta_{2j})}\right)\right], \tag{C.7}$$

where

$$Q_n(\alpha_j r)=Y'_n(\alpha_j b)J_{n+1}(\alpha_j r)-J'_n(\alpha_j b)Y_{n+1}(\alpha_j r), \tag{C.8}$$

$$M_{22,ij}=\left[\left(\frac{n(n-1)}{a^2}+\frac{\bar\delta_i^2-\bar\alpha_{2i}^2}{2}\right)J_n(\bar\alpha_{1i}a)+\frac{\bar\alpha_{1i}}{a}J_{n+1}(\bar\alpha_{1i}a),\right.$$
$$+K_{1i}\bar\delta_i\left(\bar\alpha_{2i}J_n(\bar\alpha_{2i}a)-\frac{(n+1)}{a}J_{n+1}(\bar\alpha_{2i}a)\right),\quad e=1\quad\text{for}\quad\alpha_i\neq0,$$
$$\left.+\Lambda_{1i}\bar\delta_i\left(\bar\alpha_{2i}Y_n(\bar\alpha_{2i}a)-\frac{(n+1)}{a}Y_{n+1}(\bar\alpha_{2i}a)\right)\right]\left(\frac{el}{2}\right),\quad e=2\quad\text{for}\quad\alpha_i=0, \tag{C.9}$$

$$M_{23,ij}=\left[\left(\frac{n(n-1)}{r^2}+\frac{\bar\delta_i^2-\bar\alpha_{2i}^2}{2}\right)Y_n(\bar\alpha_{1i}a)+\frac{\bar\alpha_{1i}}{a}Y_{n+1}(\bar\alpha_{1i}a)\right.$$
$$+K_{2i}\bar\delta_i\left(\bar\alpha_{2i}J_n(\bar\alpha_{2i}a)-\frac{(n+1)}{a}J_{n+1}(\bar\alpha_{2i}a)\right)$$
$$\left.+\Lambda_{2i}\bar\delta_i\left(\bar\alpha_{2i}Y_n(\bar\alpha_{2i}a)-\frac{(n+1)}{a}Y_{n+1}(\bar\alpha_{2i}a)\right)\right]\left(\frac{el}{2}\right) \tag{C.10}$$

$$M_{24,ij}=\left[\frac{n(n-1)}{a^2}J_n(\bar\alpha_{2i}a)-\frac{n\bar\alpha_{2i}}{r}J_{n+1}(\bar\alpha_{2i}a)\right.$$
$$+K_{3i}\bar\delta_i\left(\bar\alpha_{2i}J_n(\bar\alpha_{2i}a)-\frac{(n+1)}{a}J_{n+1}(\bar\alpha_{2i}a)\right)$$
$$\left.+\Lambda_{3i}\bar\delta_i\left(\bar\alpha_{2i}J_n(\bar\alpha_{2i}a)-\frac{(n+1)}{a}J_{n+1}(\bar\alpha_{2i}a)\right)\right]\left(\frac{el}{2}\right) \tag{C.11}$$

$$M_{25,ij}=\left[\frac{n(n-1)}{a^2}Y_n(\bar\alpha_{2i}a)-\frac{n\bar\alpha_{2i}}{a}Y_{n+1}(\bar\alpha_{2i}a)\right.$$
$$+K_{4i}\bar\delta_i\left(\bar\alpha_{2i}J_n(\bar\alpha_{2i}a)-\frac{(n+1)}{a}J_{n+1}(\bar\alpha_{2i}a)\right)$$
$$\left.+\Lambda_{4i}\bar\delta_i\left(\bar\alpha_{2i}Y_n(\bar\alpha_{2i}a)-\frac{(n+1)}{a}Y_{n+1}(\bar\alpha_{2i}a)\right)\right]\left(\frac{el}{2}\right), \tag{C.12}$$

$$M_{31,ij} = \sum_{j=1}^{N_1}\left[\frac{-2n}{a}\left(\frac{(n-1)}{a}P_n(\alpha_j a) - \alpha_j Q_n(\alpha_j a)\right)\right.$$
$$\left(\left(\alpha_j^2 - \delta_{2j}^2\right)\left(\frac{\sin((\bar{\delta}_i - \delta_{1j})l)}{2(\bar{\delta}_i - \delta_{1j})} + \frac{\sin((\bar{\delta}_i + \delta_{1j})l)}{2(\bar{\delta}_i + \delta_{1j})}\right)\right.$$
$$\left.\left. + 2\delta_{1j}\delta_{2j}\frac{\sin(\delta_{1j}l)}{\sin(\delta_{2j}l)}\left(\frac{\sin((\bar{\delta}_i - \delta_{2j})l)}{2(\bar{\delta}_i - \delta_{2j})} + \frac{\sin((\bar{\delta}_i + \delta_{2j})l)}{2(\bar{\delta}_i + \delta_{2j})}\right)\right)\right], \tag{C.13}$$

$$M_{32,ij} = \left[\frac{-2n}{a}\left(\frac{(n-1)}{a}J_n(\delta_i a) - \delta_i J_{n+1}(\delta_i a)\right)\right.$$
$$+ K_{1i}\bar{\delta}_i\left(\bar{\alpha}_{2i}J_n(\bar{\alpha}_{2i}a) - \frac{2(n+1)}{a}J_{n+1}(\bar{\alpha}_{2i}a)\right)$$
$$\left.+\Lambda_{1i}\bar{\delta}_i\left(\bar{\alpha}_{2i}Y_n(\bar{\alpha}_{2i}a) - \frac{2(n+1)}{a}Y_{n+1}(\bar{\alpha}_{2i}a)\right)\right]\left(\frac{el}{2}\right), \tag{C.14}$$

$$M_{33,ij} = \left[\frac{-2n}{a}\left(\frac{(n-1)}{a}Y_n(\bar{\alpha}_{1i}a) - \bar{\alpha}_{1i}Y_{n+1}(\bar{\alpha}_{1i}a)\right)\right.$$
$$+ K_{2i}\bar{\delta}_i\left(\bar{\alpha}_{2i}J_n(\bar{\alpha}_{2i}a) - \frac{2(n+1)}{a}J_{n+1}(\bar{\alpha}_{2i}a)\right)$$
$$\left.+\Lambda_{2i}\bar{\delta}_i\left(\bar{\alpha}_{2i}Y_n(\bar{\alpha}_{2i}a) - \frac{2(n+1)}{a}Y_{n+1}(\bar{\alpha}_{2i}a)\right)\right]\left(\frac{el}{2}\right), \tag{C.15}$$

$$M_{34,ij} = \left[\left(\bar{\alpha}_{2i}^2 - \frac{2n(n-1)}{a^2}\right)J_n(\bar{\alpha}_{2i}r) - \frac{2\bar{\alpha}_{2i}}{a}J_{n+1}(\bar{\alpha}_{2i}a)\right.$$
$$+ K_{3i}\bar{\delta}_i\left(\bar{\alpha}_{2i}J_n(\bar{\alpha}_{2i}a) - \frac{2(n+1)}{a}J_{n+1}(\bar{\alpha}_{2i}a)\right)$$
$$\left.+\Lambda_{3i}\bar{\delta}_i\left(\bar{\alpha}_{2i}Y_n(\bar{\alpha}_{2i}a) - \frac{2(n+1)}{a}Y_{n+1}(\bar{\alpha}_{2i}a)\right)\right]\left(\frac{el}{2}\right), \tag{C.16}$$

$$M_{35,ij} = \left[\left(\bar{\alpha}_{2i}^2 - \frac{2n(n-1)}{a^2}\right)Y_n(\bar{\alpha}_{2i}a) - \frac{2\bar{\alpha}_{2i}}{a}Y_{n+1}(\bar{\alpha}_{2i}a)\right.$$
$$+ K_{4i}\bar{\delta}_i\left(\bar{\alpha}_{2i}J_n(\bar{\alpha}_{2i}a) - \frac{2(n+1)}{a}J_{n+1}(\bar{\alpha}_{2i}a)\right)$$
$$\left.+\Lambda_{4i}\bar{\delta}_i\left(\bar{\alpha}_{2i}Y_n(\bar{\alpha}_{2i}a) - \frac{2(n+1)}{a}Y_{n+1}(\bar{\alpha}_{2i}a)\right)\right]\left(\frac{el}{2}\right), \tag{C.17}$$

$M_{4k,ij}$ and $M_{5k,ij}$ ($k = 1,2,3,4,5$) can be calculated by replacing a with b in $M_{2k,ij}$ and $M_{3k,ij}$, respectively.

Appendix D

The components of M_{st} for the first form solution of the Fixed-end circular cylinder are as follows:

$$M_{11,ij} = \left(\frac{\alpha_j^2}{\delta_{2j}}\cos(\delta_{1j}l)\tan(\delta_{2j}l) + \delta_{1j}\sin(\delta_{1j}l)\right), \qquad i = 1,2,3...N_2,$$
$$\times\frac{1}{2}\left((b^2 - a^2) + \frac{n^2(P_n^2(\alpha_j a) - P_n^2(\alpha_j b))}{\alpha_j^2}\right), \qquad j = 1,2,3...N_1, \tag{D.1}$$

$$M_{12,ij} = \sum_{i=1}^{N_2} (-1)^{i-1} \left[\bar{\delta}_i \Pi_J(\alpha_j, \bar{\alpha}_{1i}) + K_{1i} \bar{\alpha}_{2i} \Pi_J(\alpha_j, \bar{\alpha}_{2i}) + \Lambda_{1i} \bar{\alpha}_{2i} \Pi_Y(\alpha_j, \bar{\alpha}_{2i}) \right] \tag{D.2}$$

$$M_{13,ij} = \sum_{i=1}^{N_2} (-1)^{i-1} \left[\bar{\delta}_i \Pi_Y(\alpha_j, \bar{\alpha}_{1i}) + K_{2i} \bar{\alpha}_{2i} \Pi_J(\alpha_j, \bar{\alpha}_{2i}) + \Lambda_{2i} \bar{\alpha}_{2i} \Pi_Y(\alpha_j, \bar{\alpha}_{2i}) \right], \tag{D.3}$$

$$M_{14,ij} = \sum_{i=1}^{N_2} (-1)^{i-1} \left[K_{3i} \bar{\alpha}_{2i} \Pi_J(\alpha_j, \bar{\alpha}_{2i}) + \Lambda_{3i} \bar{\alpha}_{2i} \Pi_Y(\alpha_j, \bar{\alpha}_{2i}) \right], \tag{D.4}$$

$$M_{15,ij} = \sum_{i=1}^{N_2} (-1)^{i-1} \left[K_{4i} \bar{\alpha}_{2i} \Pi_J(\alpha_j, \bar{\alpha}_{2i}) + \Lambda_{4i} \bar{\alpha}_{2i} \Pi_Y(\alpha_j, \bar{\alpha}_{2i}) \right], \tag{D.5}$$

$$\begin{aligned} M_{21,ij} = \sum_{j=1}^{N_1} \Bigg[& \left(\left(\frac{n(n-1)}{r^2} + \delta_{1j}^2 - \frac{\alpha_j^2 + \delta_{2j}^2}{2} \right) P_n(\alpha_j a) + \frac{\alpha_j}{r} Q_n(\alpha_j a) \right) \\ & \times \left(\frac{\sin((\bar{\delta}_i - \delta_{1j})l)}{2(\bar{\delta}_i - \delta_{1j})} + \frac{\sin((\bar{\delta}_i + \delta_{1j})l)}{2(\bar{\delta}_i + \delta_{1j})} \right) + \frac{\cos(\delta_{1j} l)}{\cos(\delta_{2j} l)} \left(\left(\alpha_j^2 - \frac{n(n-1)}{r^2} \right) P_n(\alpha_j a) \right. \\ & \left. - \frac{\alpha_j}{r} Q_n(\alpha_j a) \right) \times \left(\frac{\sin((\bar{\delta}_i - \delta_{2j})l)}{2(\bar{\delta}_i - \delta_{2j})} + \frac{\sin((\bar{\delta}_i + \delta_{2j})l)}{2(\bar{\delta}_i + \delta_{2j})} \right) \Bigg], \end{aligned} \tag{D.6}$$

$$\begin{aligned} M_{31,ij} = \sum_{j=1}^{N_1} \Bigg[& \frac{-2n}{a} \left(\frac{(n-1)}{a} P_n(\alpha_j a) - \alpha_j Q_n(\alpha_j a) \right) \left(\left(\frac{\sin((\bar{\delta}_i - \delta_{1j})l)}{2(\bar{\delta}_i - \delta_{1j})} \right. \right. \\ & \left. \left. + \frac{\sin((\bar{\delta}_i + \delta_{1j})l)}{2(\bar{\delta}_i + \delta_{1j})} \right) - \frac{\cos(\delta_{1j} l)}{\cos(\delta_{2j} l)} \left(\frac{\sin((\bar{\delta}_i - \delta_{2j})l)}{2(\bar{\delta}_i - \delta_{2j})} + \frac{\sin((\bar{\delta}_i + \delta_{2j})l)}{2(\bar{\delta}_i + \delta_{2j})} \right) \right) \Bigg]. \end{aligned} \tag{D.7}$$

$M_{2k,ij}$ and $M_{3k,ij}$ ($k = 2,3,4,5$) can be calculated the same as given in Appendix C.
$M_{4k,ij}$ and $M_{5k,ij}$ ($k = 2,3,4,5$) can be calculated by replacing a with b in $M_{2k,ij}$ and $M_{3k,ij}$, respectively.

References

[1] L. Pochhamer, Uber die fortpflanzungsgeschwindigkeiten kleiner schwingungen in einem unbegrenzten isotropen kreiscylinder, *Zeitschrift fur Reine und Angewandte Mathematik* 81 (1876) 324–336.
[2] C. Chree, The equations of an isotropic elastic solid in polar and cylindrical coordinates, their solutions and applications, *Transactions of the Cambridge Philosophical Society* 14 (1889) 250–309.
[3] J.E. Greenspon, Flexural vibrations of a thick-walled circular cylinder according to the exact theory of elasticity, *Journal of Aero/Space Sciences* 27 (1957) 1365–1373.
[4] D.C. Gazis, Three dimensional investigation of the propagation of waves in hollow circular cylinder, *Journal of the Acoustical Society of America* 31 (1959) 568–578.
[5] A.E. Armenakas, Propagation of harmonic waves in composite circular cylindrical shells—I: Theoretical investigations, *AIAA Journal* 5 (1967) 740–744.
[6] H.D. McNiven, A.H. Shah, J.L. Sackman, Axially symmetric waves in hollow, elastic rod—part 1, *Journal of the Acoustical society of America* 40 (1966) 784–791.
[7] G.M. Gladwell, U.C. Tahbildar, Finite element analysis of axisymmetric vibrations of cylinders, *Journal of Sound and Vibration* 22 (1972) 143–157.
[8] G.M. Gladwell, D.K. Vijay, Natural frequencies of free finite length circular cylinders, *Journal of Sound and Vibration* 42 (1975) 387–397.
[9] J.R. Hutchinson, Axisymmetric vibrations of a free finite length rod, *Journal of the Acoustical Society of America* 51 (1971) 233–240.
[10] J.R. Hutchinson, Vibrations of solid cylinders, *Journal of Applied Mechanics* 47 (1980) 901–907.
[11] J.R. Hutchinson, S.A. El-Azhari, Vibrations of free hollow circular cylinders, *Journal of Applied mechanics* 53 (1986) 641–646.
[12] R.K. Singal, K. Williams, A theoretical and experimental study of vibrations of thick circular cylindrical shell and rings, *Journal of Vibration, Acoustics, Stress and Reliability in Design* 110 (1988) 533–537.

[13] A.W. Leissa, J. So, Accurate vibration frequencies of circular cylinders from three-dimensional analysis, *Journal of the Acoustical Society of America* 98 (1995) 2136–2141.
[14] J. So, A.W. Leissa, Free vibration of thick hollow circular cylinders from three-dimensional analysis, *Journal of Vibration and Acoustics* 119 (1997) 89–95.
[15] K.M. Liew, K.C. Hung, Three-dimensional vibratory characteristics of solid cylinders and some remarks of simplified beam theories, *International Journal of Solids and Structures* 32 (1995) 3499–3513.
[16] K.M. Liew, K.C. Hung, M.K. Lim, Vibration of stress free hollow cylinders of arbitrary cross-section, *Journal of Applied Mechanics, ASME* 62 (1995) 718–724.
[17] K.C. Hung, K.M. Liew, M.K. Lim, Free vibration of cantilevered cylinders: effects of cross-sections and cavities, *Acta Mechanica* 113 (1995) 37–52.
[18] H. Wang, K. Williams, Vibrational modes of thick cylinders of finite length, *Journal of Sound and Vibration* 191 (1996) 955–971.
[19] D. Zhou, Y.K. Cheung, S.H. Lo, F.T.K. Au, 3D vibration analysis of solid and hollow circular cylinders via Chebyshev–Ritz method, *Computer Methods in Applied Mechanics and Engineering* 192 (2003) 1575–1589.
[20] J.H. Lee, J. Kim, Analysis and measurement of sound transmission through a double-walled cylindrical shell, *Journal of Sound and Vibration* 251 (2002) 631–649.